

# Atomistic modeling of electric field poling of PMMA-based polymer material with guest quinoxaline chromophores

Olga D. Fominykh <sup>\*</sup>, Anastasiya V. Sharipova, Marina Yu. Balakina

Arbuzov Institute of Organic and Physical Chemistry FRC Kazan Scientific Center of Russian Academy of Sciences, Arbuzov Str. 8, 420088 Kazan, Russia



## ARTICLE INFO

### Keywords:

Atomistic modeling  
Quinoxaline chromophore orientation  
Composite polymer material  
Applied electric field  
Acentric order parameter

## ABSTRACT

The effect of applied electric field strength on the chromophore alignment in composite PMMA-based material is studied by atomistic modeling. Polymer material of real density (1.07 g/cm<sup>3</sup>), established in the course of modeling using NPT protocol, is considered along with model materials with reduced density (0.6 and 0.9 g/cm<sup>3</sup>), applied fields ranging from 100 to 1000 V/μm. Glass transition temperature, at which materials simulation was performed, was estimated in the course of multistage simulation. Simulation was performed with OPLS3e force field. Both centric,  $\langle P_2 \rangle$ , and acentric,  $\langle \cos^3 \Theta \rangle$ , chromophores order parameters were estimated. For the polymer material with high density,  $\rho = 1.07 \text{ g/cm}^3$ , the value of the order parameter  $\langle \cos^3 \Theta \rangle$  grows from 0.25 to 0.30 for field strength varying from 300 to 1000 V/μm; the values of  $\langle P_2 \rangle$  for chromophores are in agreement with the results of measurements by UV-vis spectroscopy. The obtained values of order parameters (both  $\langle P_2 \rangle$  (ch) and  $\langle \cos^3 \Theta \rangle$ ) for model materials with decreased density (0.6 and 0.9 g/cm<sup>3</sup>) are quite close to each other and seem to be overestimated compared to the values for the material with high density; this observation is in agreement with calculated values of free volume in the composite. The applied approach may provide guidelines for the elaboration of optimal poling protocols used at the development of composite polymer materials with quadratic nonlinear optical properties, containing quinoxaline chromophores-guests possessing high dipole moments (more than 20 D).

## 1. Introduction

One of the key steps in the development of polymer material with quadratic nonlinear optical (NLO) response to the applied laser field is poling, which results in the formation of noncentrosymmetric chromophores organization in the material governed by the dc field [1,2]. Optimization of poling characteristics, in particular, poling field strength, poling temperature, local mobility of chromophores and fragments of polymer chains is necessary to achieve effective chromophore reorientation. During the last decades, molecular simulation has been used to clarify the process of chromophores reorientation during poling by the example of composite polymer materials with various chromophores as guests using both statistical Monte-Carlo [3–6] and atomistic modeling approaches [7–11].

The results of Monte Carlo studies of azochromophores reorientation in polymer systems, using methods based on the bond-fluctuation model for a polymer matrix, are reviewed in [3]. The study of the effect of chromophores shape and concentration were performed in [4–6,12,13]; and the account of the effect of intermolecular interactions was

considered in [4,13]. Currently, the coarse-grained statistical Monte-Carlo approach is exploited [14–18], permitting to clarify the importance of chromophore structure modifications with respect to optimizing poling efficiency [17] and to realize the relationship between the chromophore number density, dipole moment and acentric order [18]. The special attention is paid to the prediction of EO coefficient in the framework of approaches combining simulation and quantum chemistry [15,16].

Modern simulation techniques based on molecular dynamics (MD) provide guidelines for optimization of poling parameters, permitting the estimation of the macroscopic properties of a system and the study of the microscopic origin behind them [7–11,19,20]. In a number of papers, the effect of the chromophores ordering in the composite polymer material on the value of electrooptic (EO) coefficient was studied: the effect of polymer chains local dynamics [5,7,21,22] and the free volume size and shape near the chromophore [5,7,21] on chromophores reorientation was considered; correlated motion of chromophores and polymer side groups was established [7,11]; the effect of material density was studied in [7–9].

<sup>\*</sup> Corresponding author.

E-mail address: [fod5@yandex.ru](mailto:fod5@yandex.ru) (O.D. Fominykh).

Atomistic modeling was applied exclusively to the study of chromophore alignment in the polymer composites, various chromophores, in particular, DPNA and nitrostyrene ones [11,21], azochromophores [7,10,11,23,24], EZ-FTC [8,9] and CLD-1 [4,12], YLD-156 [13] being used as guests (for full chemical names see SI). Different approaches were elaborated for the estimation of order parameters characterizing the quality of chromophores alignment [6,8–11,13,23,24]: both centric and acentric order parameters estimated with the account of intermolecular interactions and their correlation with the experiment were analyzed in [13]; the correlation between centric and acentric order parameters in terms of system dimensionality [6], the effect of the applied field strength, chromophores dipole moment and material density on the polar order parameter was considered in [8–10].

In early works, too high values of the poling fields and temperatures were used in modeling to compensate short simulation time [7–11,21]. However, at present expanded computer capabilities make it possible to perform simulations under realistic experimentally accessible conditions.

Here we present the results of the atomistic simulation of polymethyl methacrylate (PMMA)-based composite material doped with chromophores with quinoxaline moiety in  $\pi$ -electron bridge as guests (Fig. 1) [25], the chromophore content being 15 wt%. The effects of material density and poling conditions (temperature and the strength of the applied electric dc field) on the effectiveness of chromophores orientation, as well as the orientation of polar groups in polymer chains, which also contribute to the order parameter of material as a whole, are analyzed.

## 2. Computational details

The studied systems are composite polymer materials based on polymethyl methacrylate (PMMA) with quinoxaline guest chromophores, ch, with the 15 wt% content; the corresponding material is denoted as PMMA/ch(15). The degree of polymerization is chosen to be 60 units; the material is modeled by ten PMMA chains and sixteen chromophores providing 15 wt% content. Quinoxaline chromophore has large linear size ( $\sim 24$  Å) and is characterized by very high dipole moment (more than 20 D) [25].

OPLS3e force field was used with both built-in partial charges [26,27] and the ESP-charges (charges reproducing chromophore electrostatic potential) at chromophore atoms calculated at B3LYP/6-31G (d) level. The application of ESP charges permitted to get appropriate charge separation in the chromophore (charge on donor is 0.190, charge on  $\pi$ -bridge is -0.021, charge on acceptor is -0.168) contrary to the case of built-in charges (charge on D is -0.024, charge on  $\pi$ -bridge is 0.085, charge on A is -0.102). The partial charges on atoms are given in Fig. S1. Built-in OPLS3e charges were used for charge distribution description in polymer chains. Non-bonded interactions are represented by Coulomb and Lennard-Jones terms covering pairwise interactions between available interacting sites. The cutoff radius was chosen to be 9 Å. Interactions between pairs of atoms separated by greater distances are computed by the Ewald summation technique. Starting polymer chain conformation was obtained as a result of Monte-Carlo conformational search; the most stable conformation was taken for further simulation. Polymer chains and chromophores were packed into the so-called amorphous cell, the size of which was chosen to provide required

composite polymer material density: 0.61, 0.90 and 1.07 g/cm<sup>3</sup>. The amorphous cell is cubic, the cube edge length is 57.54, 50.65 and 47.8 Å respectively.

In the course of building an amorphous cell with the given density, the stage of Monte-Carlo simulated annealing was used, when the system was gradually cooled in three steps from 900 K to the desired temperature, at which the modeling was performed (900 K; 600 K; target temperature (400 K or 470 K)). This stage allowed getting the material with minimum dipole moment. The stage of MD in applied electric field was preceded by constant volume relaxation. For the systems with low density another procedure of system relaxation was used – the material was annealed (see protocol of simulated annealing in Table S1) with final desired temperature and then MD in applied electric field was performed without additional relaxation.

Free volume and its distribution in the amorphous cell were estimated for model materials with definite densities. The location and sizes of voids (free volume) in the materials were determined by a grid-based method. The results are displayed in the form of a histogram of void sizes. The size is represented by the radius of a sphere that contains the same volume as the void. The 3D images of free volume distribution were also obtained.

The glass transition temperature,  $T_g$ , was estimated in the framework of constant pressure NPT MD starting from equilibration at 600 K for 50 ns. The system was cooled from 600 to 200 K with decrement 20 K and equilibration time 20 ns at each temperature step. The value of  $T_g$  was obtained by bilinear fit as intersection of two regression lines corresponding to the specific volume (1/density) change with the temperature in low temperature (glassy) region and the high temperature (rubbery) region; alternative approach to  $T_g$  estimation is based on intersection of tangents to the hyperbola branches (hyperbolic fitting) of density dependence on temperature.

The molecular modeling was performed with Materials Science Suite complex [28], which includes Desmond engine [29] for molecular dynamics calculations of material in amorphous cell. Chromophores organization in composite polymer material is characterized by centrosymmetric,  $\langle P2 \rangle$ , and noncentrosymmetric,  $\langle \cos^3 \Theta_i \rangle$ , order parameters, describing the degree of chromophores orientation relative to the direction of the applied electric field  $\vec{E}$ .  $\langle P2 \rangle$  is estimated as

$$\langle P2 \rangle = \left( \frac{1}{N} \sum_{i=1}^N P2_i (\cos \Theta_i) P2_i \right) / 2 \quad (1)$$

$\Theta_i$  is an angle between  $\vec{E}$  and the direction of  $i$ -th chromophore dipole moment  $\mu_i$  (Fig. 2), N is a number of chromophores; the summation is performed over all chromophores dipole moments.  $\langle P2 \rangle$  does not distinguish between the direction of  $\mu$  along or against the field. According to the definition,  $\langle P2 \rangle = 1$  characterizes ideal orientation of chromophores along  $\vec{E}$ . The case  $\langle P2 \rangle = 0$  generally speaking corresponds to random (isotropic) orientation of chromophores dipole moments with respect to  $\vec{E}$  (ideal alignment at the “magic angle” 54.7°); however since  $\langle P2 \rangle$  does not distinguish between the direction of  $\mu$  along or against the field, it can be close to zero even at anisotropic chromophores arrangement.

Acentric order parameter  $\langle \cos^3 \Theta \rangle$  in the model of non-interacting rigid gas is defined as

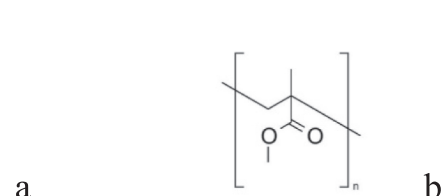
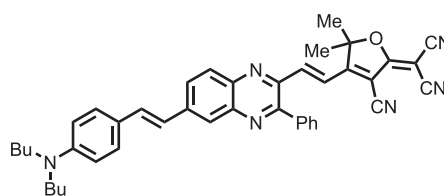


Fig. 1. Chromophore-guest with dibutylaniline donor, divinylquinoxaline bridge and tricyanofuran acceptor, (here ch), (a); PMMA monomer unit (b).

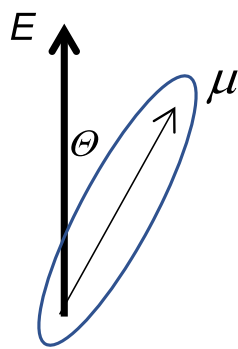


Fig. 2. Angle between dipole moment and applied electric field.

$$\langle \cos^3 \Theta \rangle = L_3(f); f = \bar{\mu} \cdot \vec{E} / kT \quad (2)$$

where  $L_3(f)$  is a third-order Langevin function; when  $f$  is small  $\langle \cos^3 \Theta \rangle \approx -f/5$  [30]. When interchromophore interactions are not negligible,  $\langle \cos^3 \Theta \rangle$  may be estimated as [31,32]:

$$\langle \cos^3 \Theta \rangle = L_3(f) \left[ 1 - L_1 \left( \frac{W}{kT} \right)^2 \right], \quad (3)$$

where  $W$  is a chromophore-chromophore interaction energy and  $L_1$  is a Langevin function. Taking into account the relation between  $\langle P_2 \rangle$  and  $\langle \cos^3 \Theta \rangle$  parameters, one may estimate acentric order parameter by the value of  $\Theta_i$  calculated from  $P_{2i}$  value; when  $P_2$  is of the order of 0.6 or greater, the difference between  $P_2$  and  $\langle \cos^3 \Theta \rangle$  becomes negligible [13].

### 3. Results and discussion

#### 3.1. Glass transition temperature

For the studied system PMMA/ch(15)  $T_g$  was calculated both with ESP charges and built-in OPLS3e charges on chromophores. The estimated values of  $T_g$ , calculated with ESP-charges on chromophores, are  $468.4 \pm 5.8$  K for bilinear fit (Fig. 3a) and  $466.4 \pm 7.8$  K for hyperbola fit (Fig. 3b). Thus, both approaches give close  $T_g$  values.

The simulation with built-in charges provides rather similar  $T_g$  for hyperbola fit –  $457.5 \pm 20.0$  K and somewhat lower value for bilinear fit –  $438.5 \pm 6.7$  K (Fig. S3). However, it is recognized that for theoretical simulations overestimation by 30 K is assumed quite acceptable for acrylate polymers [33]. The overestimation of  $T_g$  obtained in the course of the calculations with built-in charges is less pronounced, than that with ESP-charges on chromophore atoms; however, as the latter approach gives more adequate charge distribution in the chromophore, reproducing the dipole moment value, we use thus obtained  $T_g$  as poling temperature  $T_p$  (470 K) to study the process of chromophores re-orientation in the applied electric field.

### 3.2. Analysis of chromophore dynamics in the applied electric field

To study chromophore dynamics in the material, we have performed simulations for the low (0.6 and 0.9  $\text{g}/\text{cm}^3$ ) and high (1.07  $\text{g}/\text{cm}^3$ ) density materials; the latter value was obtained in the course of multi-stage modeling with compressive (NPT) protocol (Table S2). The simulation was carried out in NVT ensemble, the applied electric field strengths were 300, 500 and 1000  $\text{V}/\mu\text{m}$ .

#### 3.2.1. Low density case $\rho = 0.6 \text{ g}/\text{cm}^3$

To reduce the probability of intermolecular chromophore interactions and to facilitate chromophore orientation in the applied electric field, the model material with reduced density of 0.6  $\text{g}/\text{cm}^3$  was considered. To study the effect of the field strength on chromophores orientation for low density systems the simulation was performed at 400 K; the strengths of applied electric field were chosen to be the following: 100, 300, 500 and 1000  $\text{V}/\mu\text{m}$ ; simulation time 50 ns. Before MD simulation the system was equilibrated in the course of Simulated Annealing (SA) procedure [34] (NVT ensemble, SA protocol with final temperature 400 K; Table S1). The main reason for SA performance was to minimize the initial dipole moment of the system. Before simulation the model system was relaxed.

We have analyzed both centric  $\langle P_2 \rangle$  and acentric  $\langle \cos^3 \Theta \rangle$  order parameters;  $\langle P_2 \rangle$  was estimated for the whole cell as well as separately for chromophores and polymer chains. Actually not only chromophores dipoles contribute to the total dipole moment of the amorphous cell containing the composite polymer material, but PMMA chains as well due to the presence of a large number of polar carbonyl groups. Acentric order parameter  $\langle \cos^3 \Theta \rangle$  was estimated for chromophores from corresponding set of  $P_{2i}(\text{ch})$  (eq.1), the sign of  $\cos \Theta_i$  was determined from the dynamics of each chromophore orientation in the course of MD (MD trajectory visual analysis); evolution of each chromophore dipole moment orientation in the applied electric field was written as a .csv data file; the set of these data files was processed by a special home-written Python script to get the value of chromophore acentric order parameter.

In Fig. 4 the evolution of  $\langle P_2 \rangle$  with time recorded in the course of MD simulation with  $E = 100 \text{ V}/\mu\text{m}$  for PMMA/ch(15) is presented along with the estimated value of  $\langle \cos^3 \Theta \rangle$  for chromophores.

The graphs for  $\langle P_2 \rangle$  demonstrate that it has the average value  $\sim 0$  both for chromophores and polymer chains what can be interpreted as random orientation of dipole moments with respect to  $\vec{E}$ , since  $\langle P_2 \rangle$  does not distinguish between the dipole moment direction along and against the field direction. The account of the chromophore dipole moments direction relative to  $\vec{E}$  results in the value of  $\langle \cos^3 \Theta \rangle \sim 0.16$  (Fig. 4b), giving evidence of chromophore orientation even at such moderate field strength due to low material density. Acentric order parameter value is shown to be higher than  $\langle P_2 \rangle$ , what is repeatedly mentioned in literature [13,35].

The obtained estimations correlate with those performed for PMMA/

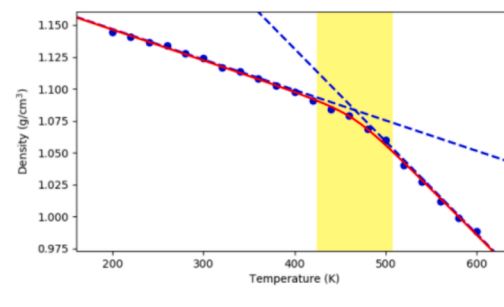
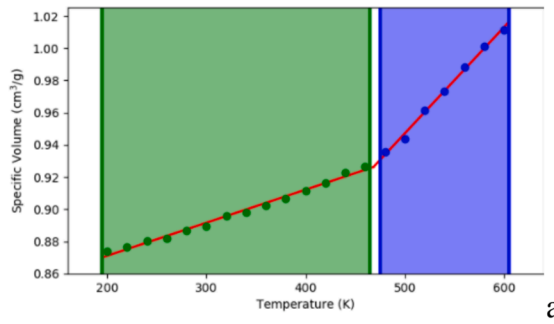
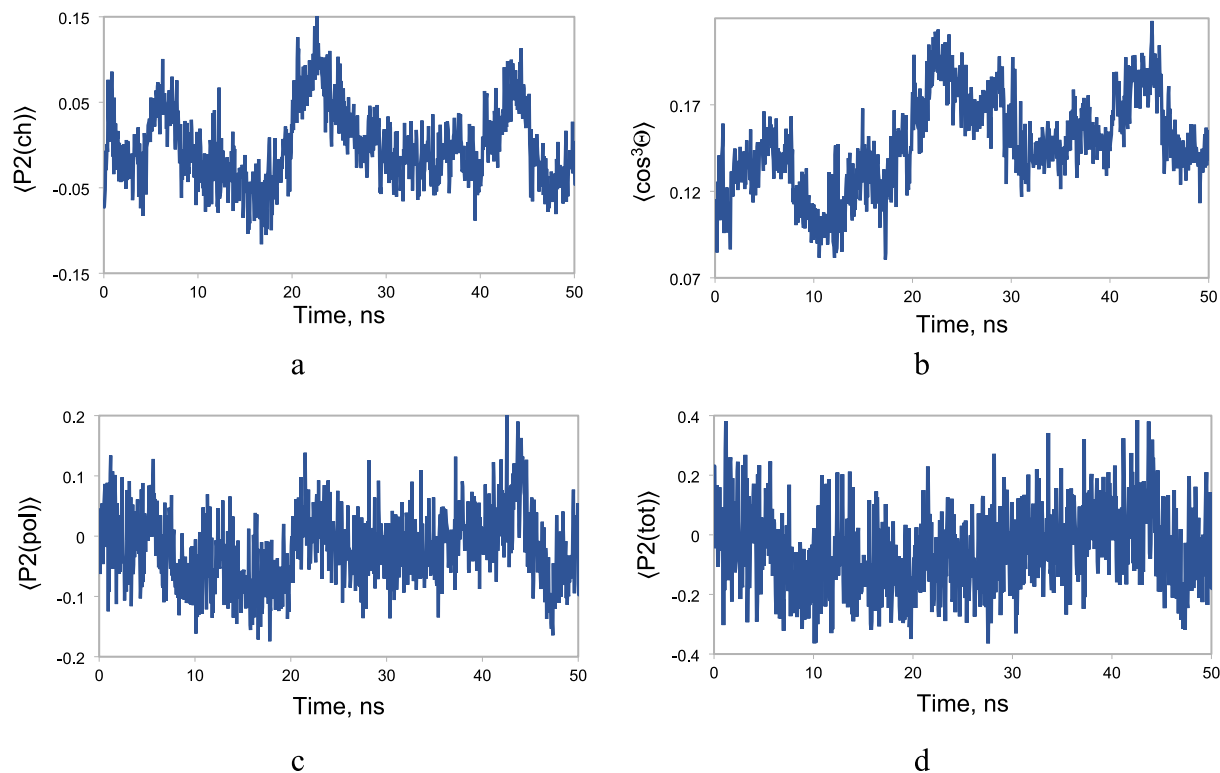


Fig. 3. The dependence of specific volume (a) and density (b) on temperature for PMMA/ch(15).



**Fig. 4.** Centric order parameter  $\langle P2(ch) \rangle$  for chromophores (a), polymer chains (c) and amorphous cell as a whole (d); acentric order parameter (b) for PMMA/ch(15);  $E_p = 100 \text{ V}/\mu\text{m}$ ;  $\rho = 0.6 \text{ g}/\text{cm}^3$ ,  $T = 400 \text{ K}$ .

F2 (F2 is an FTC-type chromophore) material with similar poling parameters ( $E_p = 75 \text{ V}/\mu\text{m}$ ,  $T_p = 382 \text{ K}$ ) at close chromophore number density ( $1.26 \cdot 10^{20} \text{ mol}/\text{cc}$  against  $0.84 \cdot 10^{20} \text{ mol}/\text{cc}$  in our case):  $\langle P2 \rangle = 0.033$  and  $\langle \cos^3\Theta \rangle = 0.082$  [13].

To study the effect of the applied field strength on the chromophores order parameters, we have repeated the simulation at higher field

strengths leaving other parameters (material density and temperature) unchanged (Fig. 5, Fig. S4).

According to the obtained results both centric and acentric order parameters essentially depend on the field strength, this observation was previously noted in literature for composites with small-size chromophores (in particular, DPNA) [9]. For our material PMMA/ch(15) with rather large chromophores (app. 25 Å length)  $\langle P2 \rangle$  and  $\langle \cos^3\Theta \rangle$  have also increased with electric field strength reaching rather high values 0.2 for  $\langle P2(ch) \rangle$  and 0.28 for  $\langle \cos^3\Theta \rangle$  already at 300 V/ $\mu\text{m}$ . Increase of field strength to  $E = 500 \text{ V}/\mu\text{m}$  resulted in quite good value of acentric order parameter – 0.33; further increase of field strength up to 1000 V/ $\mu\text{m}$  caused the growth of  $\langle \cos^3\Theta \rangle$  to 0.4. Thus for such a loose model polymer material the field strength 300 V/ $\mu\text{m}$  seems to be sufficient for effective chromophore orientation. Other simulations of polymer systems at increased temperature and with higher density were performed starting from the field strength of 300 V/ $\mu\text{m}$ .

To study the effect of temperature on chromophores orientation in the applied electric field, the simulation was repeated at 470 K (Fig. 6, Fig. S5).

The analysis of the obtained results demonstrates the growth of both  $\langle P2 \rangle$  and  $\langle \cos^3\Theta \rangle$  with temperature for the definite field strength, the corresponding values are notably higher than those for 400 K due to the enhanced chromophore mobility at increased temperature; polymer environment does not prevent chromophore orientation as material density is rather low. It is consistent with the observation, made earlier for chromophores of a smaller size. It is worth noting that even at 300 V/ $\mu\text{m}$  the acentric order parameter is very high – 0.42 (Fig. 6b); at 1000 V/ $\mu\text{m}$   $\langle \cos^3\Theta \rangle$  value is found to be 0.65 which seems to be unrealizable. Similar result was obtained for PMMA/EZ-FTC with density  $0.5 \text{ g}/\text{cm}^3$  in the course of simulation ( $E_p = 1000 \text{ V}/\mu\text{m}$ ,  $T_p = 600 \text{ K}$ ):  $\langle \cos^3\Theta \rangle$  reached  $0.6 \pm 0.07$  [9].

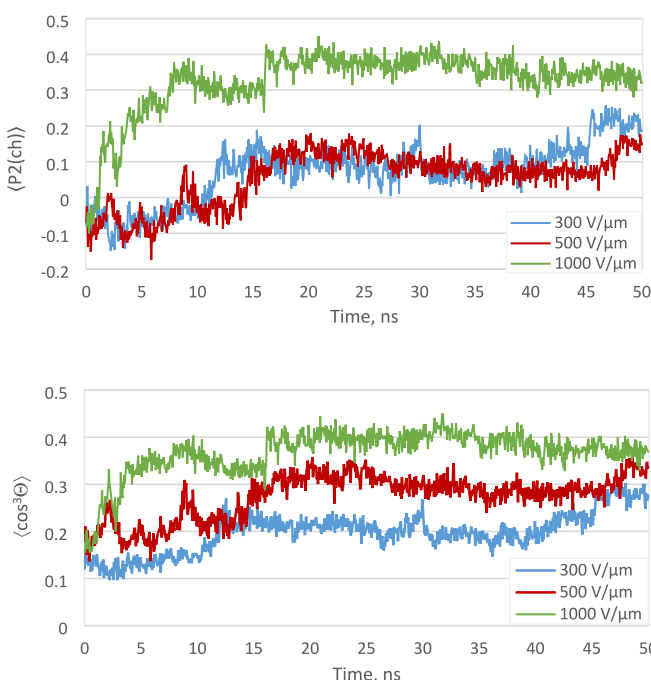


**Fig. 5.** The evolution of chromophores centric,  $\langle P2(ch) \rangle$ , and acentric,  $\langle \cos^3\Theta \rangle$ , order parameters during simulation;  $\rho = 0.6 \text{ g}/\text{cm}^3$ ,  $T = 400 \text{ K}$ .

### 3.2.2. Material density $\rho = 0.9 \text{ g}/\text{cm}^3$

The results of simulation of polymer system with the density ( $\rho = 0.9$

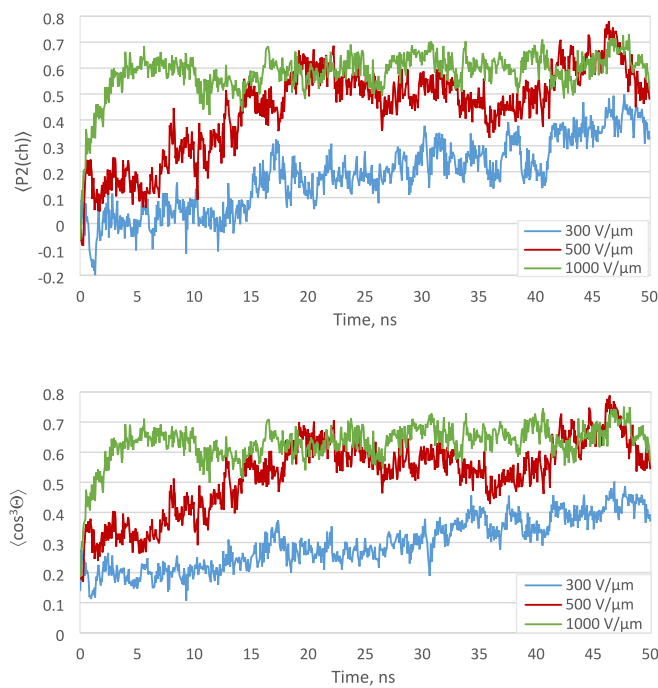


**Fig. 6.** The evolution of chromophores centric,  $\langle P2(ch) \rangle$ , and acentric,  $\langle \cos^3\Theta \rangle$ , order parameters during simulation;  $\rho = 0.6 \text{ g/cm}^3$ ,  $T = 470 \text{ K}$ .

$\text{g/cm}^3$ ) at various field strengths are summarized in Fig. 7, Fig. S6.

The analysis of the graphs obtained for  $\langle P2(ch) \rangle$  and  $\langle \cos^3\Theta \rangle$  revealed quite insignificant increase of both values compared to the case of the material with  $\rho = 0.6 \text{ g/cm}^3$  at  $470 \text{ K}$ ; somewhat more pronounced increase of  $\langle P2(\text{pol}) \rangle$  was observed (Fig. S6) for the material with  $\rho = 0.9 \text{ g/cm}^3$ . One of possible explanations for a small difference in chromophores orientation for systems with  $\rho = 0.6$  and  $\rho = 0.9 \text{ g/cm}^3$  may be that for the latter case the free volume (according to the estimation at the end of MD trajectory) remains sufficient for effective chromophore

orientation: it is app. 34 and 7 %, respectively (Fig. S7 a, b). For polar groups in polymer chains this free volume is quite enough for the reorientation along with chromophores alignment in the applied electric field. It should be noted that  $\langle \cos^3\Theta \rangle$  reaches saturation faster at increased field strength.

### 3.2.3. High density case

In search for the reasonable correspondence between modeling and experimental poling protocols, we have performed the MD simulation for composite polymer materials of a high density, determined in the course of packing the material in the amorphous cell with compressive NPT- protocol. The value  $\rho = 1.07 \text{ g/cm}^3$  was obtained and it is somewhat smaller than that of the density for PMMA polymer  $1.19 \text{ g/cm}^3$  at  $20^\circ\text{C}$  [36], since it is recognized that chromophores produce the plasticizing effect making the polymer chains motion easier. The results of the simulation are presented in Fig. 8, Fig. S8.

One can see that even at the smallest applied electric field (300 V/μm) the chromophores are rather efficiently oriented:  $\langle P2(ch) \rangle$  reaching 0.18 and  $\langle \cos^3\Theta \rangle = 0.25$ . The corresponding  $\Theta$  values are  $\sim 47.7^\circ$  and  $\sim 51^\circ$ ; the closeness of the values of average angles determined from P2 and  $\langle \cos^3\Theta \rangle$  gives evidence for rather efficient chromophores orientation along the applied electric field vector. Field strength increase to 500 V/μm results in almost the same  $\langle \cos^3\Theta \rangle$  value – 0.26; further growth of  $E_p$  to 1000 V/μm gives  $\langle \cos^3\Theta \rangle$  0.3; in these cases the angles estimated from order parameters are also quite close ( $47.3^\circ$ ,  $50.3^\circ$  and  $43.5^\circ$ ,  $48.9^\circ$ , respectively). The estimations of RMSD performed for the whole trajectory (from 0 to 50 ns) and for the trajectory part from 15 to 50 ns demonstrated inessential decrease (see Fig. S9); for both considered time intervals the smallest RMSD was observed for the case of electric field strength 300 V/μm. It should be noted that the effect of the applied field is more pronounced for polymer chains than for chromophores –  $\langle P2(\text{pol}) \rangle$  is 0.55, 0.64 and 0.80 for  $E_p = 300$ , 500 and 1000 V/μm, respectively, due to the smaller size of polar groups in methacrylic chains. Almost half-smaller values of chromophores acentric order parameters for  $\rho = 1.07 \text{ g/cm}^3$  compared to the case of  $\rho = 0.9 \text{ g/cm}^3$  may be explained by the extremely small (0.3 %) free volume estimated for the high density material (Fig. S7 c) what impedes effective chromophore orientation at the chosen temperature.

The analysis of the effect of material density on  $\langle P2 \rangle$  and  $\langle \cos^3\Theta \rangle$  demonstrates that the density increase from 0.9 to  $1.07 \text{ g/cm}^3$  results in the decrease of order parameters, thus revealing that at higher density steric hindrance prevents effective chromophores orientation. Similar observation was made in [9] by the example of PMMA/EZ-FTC.

We can note that for a composite polymer material with high density the obtained results for  $\langle P2(ch) \rangle$  are in satisfactory agreement with the results of order parameter measurements by UV-vis spectroscopy for this material ( $\sim 0.2$ – $0.3$ ) in [25]; the comparison is performed for  $\langle P2(ch) \rangle$  since it is precisely centrosymmetric order parameter that is estimated on the basis of UV-vis experiments. Since the direct estimation of acentric order parameter is not available, this validation gives grounds to assume that performed estimations of  $\langle \cos^3\Theta \rangle$  for the quinoxaline chromophores provide quite reasonable values. To demonstrate once again the validity of the used approach, we have added to the simulation protocol (after poling at increased temperature) the step of cooling from 470 to 300 K at the field switched on. As it was expected, after temperature decrease the acentric order parameter dropped insignificantly and then remained constant (0.22) during the simulation time, just in line with experimental observations. Figure S10 illustrates this behavior for the field strength 300 V.

## 4. Conclusion

The atomistic modeling of PMMA-based composite material with quinoxaline chromophores as guests is performed in the applied electric field of various strengths. Chromophore content was chosen to be 15 wt %. To get appropriate charge distribution providing chromophore dipole

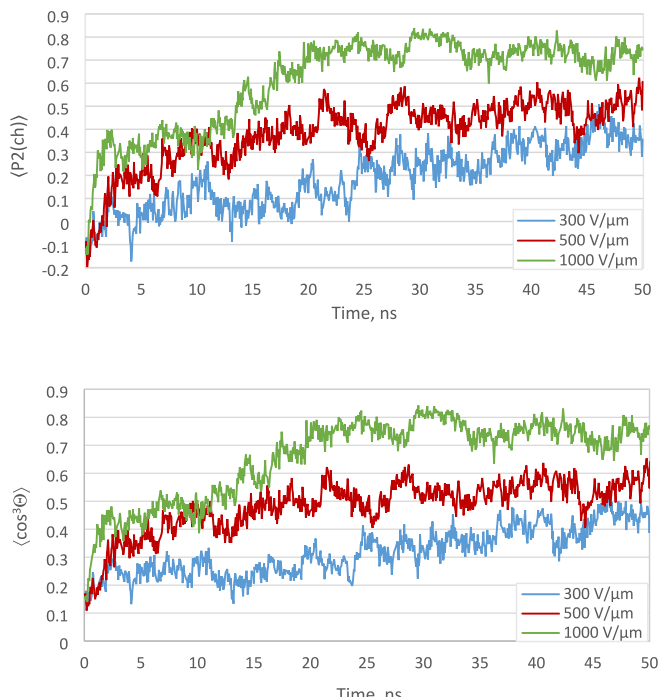


**Fig. 7.** The evolution of chromophores centric,  $\langle P2(ch) \rangle$ , and acentric,  $\langle \cos^3\Theta \rangle$ , order parameters during simulation;  $\rho = 0.9 \text{ g/cm}^3$ ,  $T = 470 \text{ K}$ .

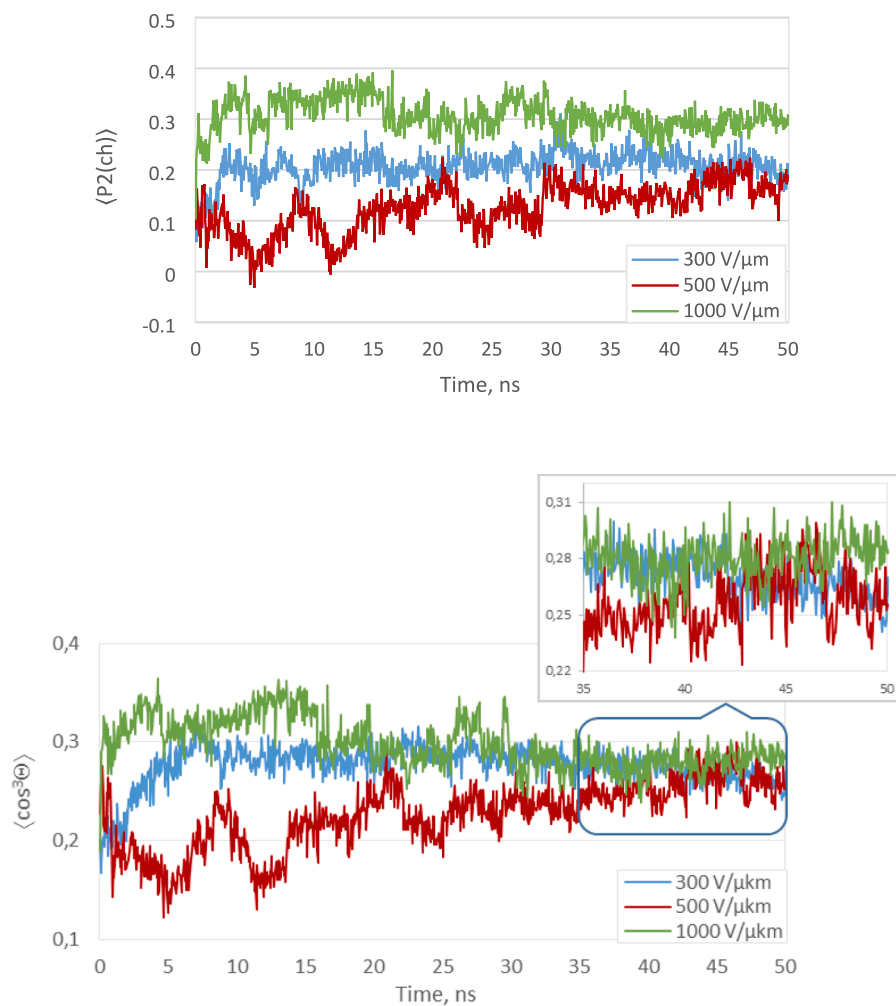


**Fig. 8.** The evolution of chromophores centric,  $\langle P2(ch) \rangle$ , and acentric,  $\langle \cos^3\Theta \rangle$ , order parameters during simulation;  $\rho = 1.07 \text{ g/cm}^3$ ,  $T = 470 \text{ K}$ .

moment ESP charges calculated at the B3LYP/6-31G(d) level were applied for the simulation, while built-in charges at the atoms of polymer chains were used. The effect of material density on the degree of chromophores orientation is studied, low ( $0.6 \text{ g/cm}^3$ ), moderate ( $0.9 \text{ g/cm}^3$ ) and high ( $1.07 \text{ g/cm}^3$ ) density cases are considered. The orientation of polar groups in polymer chains, which also contribute to the centric order parameter of material as a whole,  $\langle P2(\text{tot}) \rangle$ , is analyzed separately. Acentric,  $\langle \cos^3\Theta \rangle$ , order parameter of chromophores is estimated on the basis of  $\langle P2(ch) \rangle$  obtained from the simulation results.

We have estimated the value of  $T_g$  for the studied material which was found to be  $\sim 470 \text{ K}$ ; the simulation was performed at this temperature. The effect of temperature on the poling process was studied by the example of model polymer material of low density ( $0.6 \text{ g/cm}^3$ ); the increase of poling temperature from 400 to 470 K results in the essential growth of order parameters due to enhanced mobility of chromophores and polar groups in polymer chains.

Simulation reproduces common features of the process of chromophores orientation in the applied electric field: the value of the order parameters grows with the increase of the applied field; the considered field strengths provide effective chromophore orientation for the polymer material with  $\rho = 1.07 \text{ g/cm}^3$ , the value of  $\langle \cos^3\Theta \rangle$  ranging from 0.25 to 0.30 for  $E_p$  varying from 300 to 1000 V/μm, and the values of  $\langle P2 \rangle$  for chromophores are in agreement with the results of measurements by UV-vis spectroscopy. One may conclude that  $E_p$  300 V/μm provides good chromophores orientation in composite polymer material of high density at the temperature close to  $T_g$ ; further increase of  $E_p$  results in inessential growth of  $\langle \cos^3\Theta \rangle$ .

The obtained values of order parameters (both  $\langle P2(ch) \rangle$  and  $\langle \cos^3\Theta \rangle$ ) for model materials with decreased density ( $0.6$  and  $0.9 \text{ g/cm}^3$ ) are quite close to each other and seem to be overestimated compared to the values for the material with high density; this observation is in agreement with free volume estimations performed on the basis of the simulation results analysis.

This approach may provide guidelines for the elaboration of optimal poling protocols used at the development of composite polymer materials with quadratic NLO properties, containing chromophores-guests possessing high dipole moments (more than 20 D).

#### CRediT authorship contribution statement

**Olga D. Fominykh:** Methodology, Investigation, Formal analysis, Data curation. **Anastasiya V. Sharipova:** Investigation, Formal analysis, Data curation. **Marina Yu. Balakina:** Writing – original draft, Investigation, Funding acquisition, Conceptualization.

#### Declaration of competing interest

The authors declare that they have no known competing financial interests or personal relationships that could have appeared to influence the work reported in this paper.

#### Data availability

Data will be made available on request.

## Acknowledgements

The financial support of the Russian Science Foundation (grant no. 21-13-00206) is gratefully acknowledged.

## Appendix A. Supplementary data

Supplementary data to this article can be found online at <https://doi.org/10.1016/j.molliq.2024.125224>.

## References

- [1] D.M. Burland, R.D. Miller, C.A. Walsh, Second-order Nonlinearity in Poled-Polymer Systems, *Chem. Rev.* 94 (1994) 31–75, <https://doi.org/10.1021/cr00025a002>.
- [2] L.R. Dalton, P.A. Sullivan, D.H. Bale, Electric Field Poled Organic Electro-optic Materials: State of the Art and Future Prospects, *Chem. Rev.* 110 (2010) 25–55, <https://doi.org/10.1021/cr900429>.
- [3] A.C. Mitus, M. Saphiannikova, W. Radossz, V. Toshchevikov, G. Pawlik, Modeling of Nonlinear Optical Phenomena in Host-Guest Systems Using Bond Fluctuation Monte Carlo Model, A Review, *Materials* 14 (2021) 1454–1545, <https://doi.org/10.3390/ma14061454>.
- [4] B.H. Robinson, L. Dalton, Monte Carlo Statistical Mechanical Simulations of the Competition of Intermolecular Electrostatic and Poling Field Interactions in Defining Macroscopic Electro-Optic Activity for Organic Chromophore/Polymer Materials, *J. Phys. Chem.* 104 (2000) 4785–4795, <https://doi.org/10.1021/jp993873s>.
- [5] H.L. Rommel, B.H. Robinson, Orientation of Electro-optic Chromophores under Poling Conditions: A Spheroidal Model, *J. Phys. Chem. C* 111 (2007) 18765–18777, <https://doi.org/10.1021/jp0738006>.
- [6] B.H. Robinson, L.E. Johnson, B.E. Eichinger, Relation of System Dimensionality and Order Parameters, *J. Phys. Chem. B* 119 (2015) 3205–3212, <https://doi.org/10.1021/jp507736r>.
- [7] W.K. Kim, L.M. Hayden, Fully atomistic modeling of an electric field poled guest-host nonlinear optical polymer, *J. Chem. Phys.* 111 (1999) 5212–5222, <https://doi.org/10.1063/1.479776>.
- [8] M.R. Leahy-Hoppa, P.D. Cunningham, J.A. French, L.M. Haeden, Atomistic Molecular Modeling of the Effect of Chromophore Concentration on the Electro-optic Coefficient in Nonlinear Optical Polymers, *J. Phys. Chem. A* 110 (2006) 5792–5797, <https://doi.org/10.1021/jp0565397>.
- [9] M.R. Leahy-Hoppa, J.A. French, P.D. Cunningham, L.M. Hayden, Atomistic Molecular Modeling of Electric Field Poling of Nonlinear Optical Polymers. In: Papadopoulos, M.G., Sadlej, A.J., Leszczynski, J. (eds) Non-Linear Optical Properties of Matter. Challenges and Advances in Computational Chemistry and Physics, 2006, vol 1, pp. 337–357. Springer, Dordrecht. Doi: 10.1007/1-4020-4850-5\_11.
- [10] M. Makowska-Janusik, H. Reis, M.G. Papadopoulos, I.G. Economou, N. Zacharopoulos, Molecular Dynamics Simulations of Electric Field Poled Nonlinear Optical Chromophores Incorporated in a Polymer Matrix, *J. Phys. Chem. B* 108 (2004) 588–596, <https://doi.org/10.1021/jp036197+>.
- [11] M. Makowska-Janusik, H. Reis, M.G. Papadopoulos, I.G. Economou, Peculiarities of electric field alignment of nonlinear optical chromophores incorporated into thin film polymer matrix, *Theor. Chem. Acc.* 114 (2005) 153–158, <https://doi.org/10.1007/s00214-005-0656-x>.
- [12] P. Acebal, L. Carretero, S. Blaya, Role of Multipole Moments in Electric-Field-Induced Order of Dense Molecular Systems, *ChemPhysChem* 11 (2010) 2158–2166, <https://doi.org/10.1002/cphc.201000039>.
- [13] S.J. Benight, L.E. Johnson, R. Barnes, B.C. Olbricht, D.H. Bale, P.J. Reid, B. E. Eichinger, L.R. Dalton, P.A. Sullivan, B.H. Robinson, Reduced Dimensionality in Organic Electro-Optic Materials: Theory and Defined Order, *J. Phys. Chem. B* 114 (2010) 11949–11956, <https://doi.org/10.1021/jp1022423>.
- [14] A.F. Tillack, L.E. Johnson, M. Rawal, L.R. Dalton, B.H. Robinson, Modeling chromophore order: A Guide for improving EO performance, *MRS Online Proceedings Library* 1698 (2014), <https://doi.org/10.1557/opl.2014.795>.
- [15] B. Zerulla, D. Beutel, Ch. Holzer, I. Fernandez-Corbaton, C. Rockstuhl, M. Krstic, A Multi-Scale Approach to Simulate the Nonlinear Optical Response of Molecular Nanomaterials, *Adv. Mater.* 36 (2024) 2311405, <https://doi.org/10.1002/adma.202311405>.
- [16] M. Rawal, K.E. Garrett, L.E. Johnson, W. Kaminsky, E. Jucov, D.P. Shelton, T. Timofeeva, B.E. Eichinger, A.F. Tillack, B.H. Robinson, D.L. Elder, L.R. Dalton, Alternative bridging architectures in organic nonlinear optical materials: comparison of  $\pi$ - and  $\chi$ -type structures, *JOSA B* 33 (2016) E160–E170, <https://doi.org/10.1364/JOSAB.33.00E160>.
- [17] D.L. Elder, L.E. Johnson, A.F. Tillack, B.H. Robinson, Ch. Haffner, W. Heni, C. Hoessbacher, Y. Fedoryshyn, Y. Salamin, B. Baeuerle, A. Josten, M. Ayata, U. Koch, J. Leuthold, Larry R. Dalton, Multi-scale theory-assisted, nano-engineering of plasmonic-organic hybrid electro-optic device performance, *Proc. of SPIE* 10529 (2017) 105290K. doi: 10.1117/12.2295449.
- [18] D.L. Elder, L.R. Dalton, Organic Electro-Optics and Optical Rectification: From Mesoscale to Nanoscale Hybrid Devices and Chip-Scale Integration of Electronics and Photonics, *Ind. Eng. Chem. Res.* 61 (2022) 1207–1231, <https://doi.org/10.1021/acs.iecr.1c03836>.
- [19] T.N. Ramos, S. Canuto, B. Champagne, Unraveling the Electric Field-Induced Second Harmonic Generation Responses of Stilbazolium Ion Pairs Complexes in Solution Using a Multiscale Simulation Method, *Chem. Inf. Model.* 60 (2020) 4817–4826, <https://doi.org/10.1021/acs.jcim.9b01161>.
- [20] M.A.F. Afzal, A.R. Browning, A. Goldberg, M.D. Halls, J.L. Gavartin, T. Morisato, T. F. Hughes, D.J. Giesen, D.J. Goose, High-Throughput Molecular Dynamics Simulations and Validation of Thermophysical Properties of Polymers for Various Applications, *ACS Appl. Polym. Mater.* 3 (2021) 620–630, <https://doi.org/10.1021/acsapm.0c00524>.
- [21] J.A. Young, B.L. Farmer, J.A. Hinkley, Molecular modeling of the poling of piezoelectric polyimides, *Polymer* 40 (1999) 2787–2795, [https://doi.org/10.1016/S0032-3861\(98\)00474-1](https://doi.org/10.1016/S0032-3861(98)00474-1).
- [22] P.M. Wallace, D.R.B. Sluss, L.R. Dalton, B.H. Robinson, P.J. Reid, Single-Molecule Microscopy Studies of Electric-Field Poling in Chromophore-Polymer Composite Materials, *J. Phys. Chem. B* 110 (2006) 75–82, <https://doi.org/10.1021/jp0546711>.
- [23] Y. Tu, Y. Luo, H. Ågren, Molecular Dynamics Simulations applied to electric field induced second harmonic generation in dipolar chromophore solutions, *J. Phys. Chem. B* 110 (2006) 8971–8977, <https://doi.org/10.1021/jp0603583>.
- [24] Y. Tu, Q. Zhang, H. Ågren, Electric Field Poled Polymeric Nonlinear Optical Systems: Molecular Dynamics Simulations of Poly(methyl methacrylate) Doped with Disperse Red Chromophores, *J. Phys. Chem. B* 111 (2007) 3591–3598, <https://doi.org/10.1021/jp0673841>.
- [25] A.A. Kalinin, S.M. Sharipova, T.I. Burganov, A.I. Levitskaya, O.D. Fominykh, T. A. Vakhonina, N.V. Ivanova, A.R. Khamatgalimov, S.A. Katsuya, M. Yu. Balakina, Large nonlinear optical activity of chromophores with divinylquinoxaline conjugated  $\pi$ -bridge, *J. Photochem. & Photobiol. A*, *Chemistry* 370 (2019) 58–66, <https://doi.org/10.1016/j.jphotochem.2018.10.034>.
- [26] E. Harder, W. Damm, J. Maple, C. Wu, M. Reboul, J.Y. Xiang, L. Wang, D. Lupyan, M.K. Dahlgren, J.L. Knight, J.W. Kaus, D.S. Cerutti, G. Krilov, W.L. Jorgensen, R. Abel, R.A. Friesner, OPLS3: a force field providing broad coverage of drug-like small molecules and proteins, *J. Chem. Theory Comput.* 12 (2016) 281–296.
- [27] A.D. Bochevarov, E. Harder, T.F. Hughes, J.R. Greenwood, D.A. Braden, D. M. Philipp, D. Rinaldo, M.D. Halls, J. Zhang, R.A. Friesner, Jaguar: A high-performance quantum chemistry software program with strengths in life and materials sciences, *Int. J. Quant. Chem.* 113 (2013) 2110–2142, <https://doi.org/10.1002/qua.24481>.
- [28] Materials Science Suite, Schrodinger Release 2020–3: Schrodinger, LLC, New York, NY, 2020.
- [29] Schrodinger Release 2020–3: Desmond Molecular Dynamics System, D. E. Shaw Research, New York, NY, Maestro-Desmond Interoperability Tools, Schrodinger, New York, NY, 2020, p. 2020.
- [30] A. Piekara, A theory of electric polarization, electro-optical Kerr effect and electric saturation in liquids and solutions, *Proc. Roy. Soc. A* 172 (1939) 360–379, <https://doi.org/10.1098/rspa.1939.0109>.
- [31] L.R. Dalton, A.W. Harper, B.H. Robinson, The role of London Forces in Defining Noncentrosymmetric Order of High Dipole Moment-High Hyperpolarizability Chromophores in Electrically Poled Polymeric Thin Films, *Proc. Natl. Ac. Sci. USA* 94 (1997) 4842–4847. <https://www.jstor.org/stable/42411>.
- [32] L.R. Dalton, S.J. Benight, L.E. Johnson, D.B. Knorr, I. Kosilkina, B.E. Eichinger, B. H. Robinson, A.-K.-Y. Jen, R.M. Overney, Systematic Nanoengineering of Soft Matter Organic Electro-optic Materials, *Chem. Mater.* 23 (2011) 430–445, <https://doi.org/10.1021/cm102166j>.
- [33] J. Bicerano, Prediction of Polymer Properties, third edition., Marcel Dekker, New York, 2002, p. 784.
- [34] A. Khachaturyan, S. Semenovsovskaya, B. Vainshtein, The thermodynamic approach to the structure analysis of crystals, *Acta Crystallogr. A* 37 (5) (1981) 742–754.
- [35] B.C. Olbricht, P.A. Sullivan, P.C. Dennis, J.T. Hurst, L.E. Johnson, S.J. Benight, J. A. Davies, A. Chen, B.E. Eichinger, P.J. Reid, L.R. Dalton, B.H. Robinson, Measuring order in contact-poled organic electro-optic materials with variable angle polarization-referenced absorption spectroscopy (VAPRAS), *J. Phys. Chem. B* 115 (2011) 231–241, <https://doi.org/10.1021/jp107995t>.
- [36] G. Wypych, Handbook of polymers, Second edition, Chem.Tec. Publishing, 2016. pp. 680. Doi: 10.1016/C2015-0-01462-9.